1	Title: Sources and upstream pathways of the densest overflow water in the Nordic Seas		
2			
3	Authors: Jie Huang ^{1,2,*} , Robert S. Pickart ² , Rui Xin Huang ² , Peigen Lin ² , Ailin Brakstad ³ , and		
4	Fanghua Xu^1		
5			
6	Affiliations:		
7	¹ Ministry of Education Key Laboratory for Earth System Modeling, and Department of Eart		
8	System Science, Tsinghua University, Beijing, China		
9	² Woods Hole Oceanographic Institution, Woods Hole, USA		
10	³ Geophysical Institute, University of Bergen, and Bjerknes Centre for Climate Research, Bergen		
11	Norway		
12			
13	*Corresponding author: huangj15@mails.tsinghua.edu.cn		
14			
15	December 2019		
16	Submitted to Nature Geoscience		

The overflow water from the Nordic Seas comprises the deepest limb of the Atlantic Meridional Overturning Circulation, yet questions remain as to where it is ventilated and how it progresses to the Greenland-Scotland Ridge. Here we use historical hydrographic data from 2005-2015, together with satellite altimeter data, to elucidate the source regions of the Denmark Strait and Faroe Bank Channel overflows and the pathways by which the dense water reaches the respective sills. A recently-developed metric is used to calculate how close two water parcels are to each other in terms of physical properties, based on potential density and potential spicity. This reveals that the Greenland Sea gyre is the primary wintertime source region for the densest portion of both overflows. After subducting, the water progresses southward along several ridge systems towards the Greenland-Scotland Ridge. These inferred flow paths are confirmed using absolutely-referenced circulation maps. Extending the calculation back to the 1980s reveals that the ventilation occurred previously along the periphery of the Greenland Sea gyre, but that the pathways to the south remained the same.

1. Introduction

The overflows from the Nordic Seas feed the lower limb of the Atlantic Meridional Overturning Circulation (AMOC), which helps regulate Earth's climate. There are two general classes of overflow water¹: (1) "Atlantic-origin" overflow water which is formed by strong air-sea heat loss along the rim current system of the Nordic Seas²; and (2) "Arctic-origin" overflow water which stems from the interior basins of the western Nordic Seas where water mass transformation takes place via open-ocean convection³. The East Greenland Current (EGC) transports Atlantic-origin water to Denmark Strait, while the North Icelandic Jet (NIJ) advects a comparable amount of the denser Arctic-origin water to the strait^{3,4,5} (Fig. 1). The leading hypothesis is that the NIJ

sources from the Iceland Sea, as the lower limb of a local overturning cell³. Both types of overflow water also enter the North Atlantic through the Faroe Bank Channel^{6,7}. Previous studies suggest that the deep water formed in the Greenland Sea, and a local overturning loop within the Norwegian Sea, supply this overflow^{8,9}. To date, however, consensus has not been reached regarding the origin and upstream pathways of the densest component of the overflow water, which ventilates the deepest layers of the North Atlantic.

Water denser than 27.8 kg m⁻³ (potential density referenced to the sea surface, σ_0) is generally identified as overflow water¹⁰. The Arctic-origin overflow, found in the deepest part of Denmark Strait and the Faroe Bank Channel, is characterized by $\sigma_0 \geq 28.03$ kg m⁻³ and θ (potential temperature) ≤ 0 °C ^{3,11}. Using data from a large number of shipboard surveys, an Arctic-origin overflow transport mode of the NIJ was identified, where the bulk of the transport is confined to a small region in potential temperature-salinity (θ -S) space⁵. This mode is centered near -0.27 °C in potential temperature and 34.91 in practical salinity, corresponding to $\sigma_0 = 28.05$ kg m⁻³ and accounting for 26% of the total overflow transport⁵. By comparison, at the Faroe Bank Channel sill the densest component ($\theta \leq 0$ °C) contributes to more than half of the total overflow transport¹¹. This component has almost the same properties ($\overline{\sigma_0} = 28.05$ kg m⁻³, $\overline{\theta} = -0.4$ °C and $\overline{S} = 34.91$) as the transport mode of the NIJ. The similarity of the hydrographic properties of these two dense modes suggests a common source.

2. Applying a new metric to trace the source of the densest overflow water

We use a comprehensive historical hydrographic dataset of the Nordic Seas, described in the Methods section, to elucidate the source regions and pathways of the Arctic-origin overflow water feeding Denmark Strait and the Faroe Bank Channel. A recently-developed metric, referred to as

the σ_0 - π_0 distance, is used to calculate how close two different water parcels are to each other in terms of physical properties, where σ_0 is potential density and π_0 is potential spicity¹². The metric is effective because the isolines of potential density are orthogonal to the isolines of potential spicity, and their gradients have the same magnitude (see the Methods section). The Arctic-origin overflow water is defined by the transport mode of the NIJ in σ_0 - π_0 space, σ_0 = 28.05 kg m⁻³ and π_0 = -3.11 kg m⁻³ (the results are nearly indistinguishable using the σ_0 - π_0 values of the densest Faroe Bank Channel overflow water). Computationally, we calculate the σ_0 - π_0 distance between the water parcels in question upstream of the Greenland-Scotland Ridge and the NIJ transport mode. We consider the time period 2005-2015 to avoid effects of decadal variability, which are addressed in the last section of the paper.

We begin by asking, where in the Nordic Seas are the late-winter surface properties most closely aligned with the Arctic-origin overflow water? To answer this we determined the mixed-layer characteristics (temperature, salinity, density and depth) for approximately 8600 late-winter (February to April) profiles, using a multi-step procedure¹³. Not surprisingly, the deepest and densest mixed layers are found within the Greenland Sea gyre due to the strong atmospheric forcing and weak stratification there^{14,15} (Supplementary Fig. 1). The Iceland Sea gyre also stands out as a region of deep, dense mixed layers, but to a lesser extent than the Greenland Sea. Notably, the smallest σ_0 - π_0 distances associated with the mixed layers (as small as 0.005 kg m⁻³) are found in the Greenland Sea (Fig. 2a), indicating that this is the major source region of the densest overflow water entering the North Atlantic. A second region of relatively small σ_0 - σ_0 distances occurs in the northwest portion of the Iceland Sea, consistent with the notion that this region can supply some of the Arctic-origin overflow water to the NIJ^{16,17}. Our results imply, however, that the Iceland Sea source is relatively minor (Fig. 2a).

To elucidate the connection between the formation region of the Arctic-origin overflow and the presence of this water in Denmark Strait and the Faroe Bank Channel, we calculated the σ_0 - π_0 distances at different depth horizons in the Nordic Seas using the year-round hydrographic profiles. This reveals where the water is present after late-winter subduction. Fig. 2b shows the σ_0 - π_0 distance distribution between 250-300 m, which is the depth range of the maximum velocity in the NIJ¹⁸. The smallest σ_0 - π_0 distances still occur in the Greenland Sea. However, a potential pathway of the Arctic-origin overflow water emerges from this map. In particular, small σ_0 - σ_0 distances stem southward from the Greenland Sea along the Mohn Ridge, across the West Jan Mayen Ridge into the Iceland Sea, then along the Kolbeinsey Ridge – ultimately progressing into Denmark Strait via the NIJ. Note that no small σ_0 - π_0 distances are found along the slope of Greenland, confirming that Arctic-origin overflow water is not advected by the East Greenland Current in this depth range.

The lateral distribution of σ_0 - π_0 distances in the 600-650 m layer, near the sill depth of Denmark Strait, is generally consistent with the shallower layer (Fig. 2c). However, there are two notable differences. First, small σ_0 - π_0 distances now extend eastward along the northern slope of the Iceland-Faroe Ridge into the Faroe Bank Channel. Second, there are two bands of small values on either side of the Iceland Sea: one along the eastern side of the Kolbeinsey Ridge (similar to that seen in the shallower layer), and the other along the Jan Mayen Ridge. This suggests that, at this deeper depth horizon, two potential pathways exist carrying Arctic-origin overflow water from the Greenland Sea to the Faroe Bank Channel along the north-south ridges bounding the Iceland Sea. The σ_0 - π_0 distance map for the depth range of the Faroe Bank Channel sill (800-850 m) is qualitatively similar to that in Fig. 2c. When using the Faroe Bank Channel transport mode instead of the NIJ transport mode to compute the σ_0 - π_0 distances, the Jan Mayen Ridge pathway is even more evident in this depth range (not shown).

As a metric of the vertical structure of the σ_0 - π_0 distances, in Fig. 2d we plot the shallowest depth at which the value equals 0.05 kg m⁻³ (which is the threshold used in Figs. 2a-c to define small σ_0 - π_0 distances). This map also reveals the pathways discussed above for Arctic-origin water to progress from the Greenland Sea gyre to the two overflows. Interestingly, it implies as well that the small σ_0 - π_0 distance signal stays at roughly the same depth approaching Denmark Strait in the NIJ, but that it deepens approaching the Faroe Bank Channel along the Iceland-Faroe Ridge. Also in Fig. 2d one sees that the shallowest depth of small σ_0 - π_0 distances along the east coast of Greenland is deeper than the sill depth of Denmark Strait (650 m). This implies that the Arctic-origin water located below the Atlantic-origin water in the EGC is too deep to contribute to the densest Denmark Strait overflow. However, there is evidence of aspiration of Arctic-origin water just upstream of the sill¹⁹.

3. Upstream overflow pathways derived from composite sections

The distributions of σ_0 - π_0 distances presented above suggest that the Arctic-origin overflow water crossing the Greenland-Scotland Ridge at Denmark Strait and the Faroe Bank Channel originates primarily from the Greenland Sea, and that there are topographically-steered pathways by which the water progresses from the Greenland Sea gyre to the vicinity of the ridge. We now present kinematic evidence of these pathways using the historical hydrographic data in conjunction with satellite absolute dynamic topography data. We focus on five composite sections (Fig. 3a) that cross the ridge systems as well as the Iceland and Greenland Sea gyres, chosen to resolve the circulation in question.

Relative geostrophic velocities are computed using the hydrographic data, then referenced using the mean gridded surface geostrophic velocity field obtained from satellite altimeter data

(see the Methods section). The surface geostrophic vectors show the major currents in the study region (Fig. 3b). The two branches of the Norwegian Atlantic Current (NAC) flow northward, with the western branch turning to the northeast along the Mohn Ridge on the eastern side of the Greenland Sea gyre. The southward-flowing EGC is evident, as is the North Icelandic Irminger Current (NIIC) flowing around the north side of Iceland. There is relatively little surface signature of the Greenland Sea gyre nor the Iceland Sea gyre.

The first two composite sections (S1 and S2) reveal the cold near-surface water in the center of the Greenland Sea gyre (Fig. 3c and d). The strongly sloped isopycnals on the western side are associated with the EGC, while those on the eastern side are associated with the NAC. The flat isopycnals between the two fronts are consistent with the weak surface flow of the gyre. The third composite section (S3) is south of the Greenland Sea gyre, but still shows the strong EGC and NAC fronts. The last two composite sections (S4 and S5) pass through the northern and central portions of the Iceland Sea gyre, respectively. Here the NAC front is not associated with the eastern edge of the gyre, but is found farther to the east. However, the EGC abuts the western side of the gyre, as it did for the Greenland Sea.

We present the calculated circulation at three depth horizons: the surface, 300 m, and 650 m (Fig. 4). The latter two levels correspond to the σ_0 - π_0 distance maps in Fig. 2b and c, respectively. At the surface (Fig. 4a) the warm NAC flows northward east of the Mohn Ridge (as was noted earlier in Fig. 3b-d). The hydrographic front of the NAC is associated with strong thermal wind shear, which is large enough to reverse the circulation at 300 m and deeper (sections S2 and S3 in Fig. 4b and c). This provides a pathway of Arctic-origin overflow water away from the Greenland Sea gyre that continues southward on eastern side of the Iceland Sea along the Jan Mayen Ridge (sections S4 and S5 in Fig. 4b and c). The circulation maps also reveal a second dense water

pathway that emerges at section S2 west of the Mohn Ridge and strengthens by section S3. This branch passes through the West Jan Mayen Ridge and flows southward in the Iceland Sea on the eastern side of the Kolbeinsey Ridge (sections S4 and S5, Fig. 4b and c). Overall, these circulation pathways are consistent with the σ_0 - π_0 distance distributions presented above, including the two bands of low σ_0 - π_0 distance on the two sides of the Iceland Sea (Fig. 2c).

The two branches of Arctic-origin overflow water emanating from the vicinity of the Mohn Ridge appear to be dynamically distinct. The western branch is nearly barotropic, with a signature at the sea surface starting at section S3 (Fig. 4a and supplementary Fig. 3). In contrast, the eastern branch is sub-surface intensified with stronger flow at 650 m (Fig. 4c and supplementary Fig. 3). The fate of these two branches remains to be determined. Previous mooring data have suggested the presence of a bottom intensified current progressing eastward along the Iceland-Faroe Ridge, presumably supplying the Faroe Bank Channel overflow²⁰. It is likely that the two branches of Arctic-origin overflow water identified here feed both the NIJ and this current, but the precise partitioning and manner in which this happens needs to be worked out. Notably, the suggested pathways presented here are consistent with a two-layer modeling study²¹ and a tracer release experiment²².

4. Long-term variation in the source of the densest overflow water

We now consider the complete time period of the historical hydrographic observations to address long-term differences in the source of the Arctic-origin overflow water to the Greenland-Scotland Ridge. We focus on the densest overflow water ($28.03 \le \sigma_0 \le 28.06 \text{ kg m}^{-3}$, $\theta \le 0$ °C, and depth $\le 850 \text{m}$) in four geographical regions: the Greenland Sea gyre water (GSW), Mohn Ridge water (MRW), North Iceland slope water (ISW), and East Faroes water (EFW). These four regions

are outlined in Figure 5b. The characteristics of the NIJ water have varied by more than 0.3 °C in temperature and 0.02 in salinity from 1990 to the present¹⁷. Here we use the densest ISW water as a proxy for the time-varying NIJ transport mode; in particular, a 3-year running mean of the corresponding hydrographic properties within the ISW box over the 30-year hydrographic record (1986-2015). The equivalent timeseries for the EFW box is used for the Faroe Bank Channel transport mode (unsurprisingly, the two curves are very similar). Following this, we constructed timeseries of σ_0 - π_0 distances between the GSW and the two transport modes, as well as the MRW and the two modes (Fig. 5a). This reveals a marked increase in σ_0 - π_0 distance between the water in the center of the Greenland Sea gyre and the water feeding the two overflows prior to 2007. In contrast, the MRW has remained very close in hydrographic characteristics to the two transport modes (Fig. 5a).

This result suggests that there has been a shift in the origin of the densest water feeding the overflows, from the periphery of the Greenland Sea gyre to its center, after 2007. This is supported by the lateral map of σ_0 - π_0 distances in the 600-650 m layer from 1986-2004, i.e. prior to the time period considered in the above analysis (2005-15) (compare Fig. 5b to 2c). During both time periods, however, the pathways of small σ_0 - π_0 distances remain the same: from the Mohn Ridge into the Iceland Sea, then along the Jan Mayen and Kolbeinsey Ridges on the eastern and western sides of the Iceland Sea, respectively. The earlier period map suggests a contribution to the Faroe Bank Channel overflow from the southern half of the Norwegian Basin as well.

Why was the Greenland Sea gyre not the primary dense water source during the early time period? This is due to the change in convection within the gyre over the 30-year record. The vertical distribution of σ_0 - π_0 distance in the GSW box (Fig. 5c) shows values < 0.05 kg m⁻³ spanning the top 1000 m starting around 2007 (with small values extending to the surface

seasonally in winter). This is associated with warming of the ventilated water in the gyre due to the weakening of deep convection, and salinification of the inflowing Atlantic water into the Nordic Seas^{15,23}. Prior to 2007, the dense wintertime product in the center of the gyre was too cold and fresh to match closely the properties of the two overflow transport modes. This change in source region from outside the gyre to within the gyre likely has ramifications regarding the dynamical processes and timescale for newly ventilated water to progress from the formation region to the pathways supplying the overflows.

5. Implications and Remaining Questions

198

199

200

201

202

203

204

205

206

207

208

209

210

211

212

213

214

215

216

217

218

219

220

In this study we have elucidated the source and upstream pathways of the densest Arctic-origin water suppling the Denmark Strait and Faroe Bank Channel overflows, using a new metric for determining how close water parcels are to each other in terms of hydrographic properties. The inferred pathways were confirmed using absolutely-referenced circulation maps. Our results establish the Greenland Sea as the primary region of ventilation for the deepest layers of the North Atlantic, and reveal the importance of topographically steered pathways in channeling the dense water towards the Greenland-Scotland Ridge. This puts us in a position to understand better the link between atmospheric forcing and the densest component of the AMOC, and how this might be impacted by ongoing changes in the climate of the high latitude North Atlantic. Our study also raises several new questions, including: How and why does the newly-convected water enter the deep Mohn Ridge boundary current system after it is subducted? And how does this dense water subsequently pass through the West Jan Mayen Ridge into the Iceland Sea? Finally, it remains unknown how the dense Arctic-origin water ultimately feeds the westward-flowing NIJ and eastward-flowing current along the Iceland-Faroe Ridge. These questions need to be addressed with future observational and modeling studies.

221 Methods

The hydrographic data used in this study cover the time period 1986-2015 and the spatial domain 59°-80°N and 30°W-20°E. The majority of the data were obtained from the Unified Database for Arctic and Subarctic Hydrography (UDASH)²⁴. Additional data, particularly south of 65°N which is outside the domain of UDASH, come from various archives as listed in supplementary Table 1. All of the data were combined into a single hydrographic dataset, where duplicates between the different archives were removed. In addition to the quality control already performed on each data source, we required that all vertical profiles include both temperature and salinity. We excluded measurements outside the expected range in the Nordic Seas [-2°C, 20°C] and [20, 36] for potential temperature and practical salinity, respectively. Data with density inversions exceeding 0.05 kg m⁻³ were also excluded, except when the inversion was associated with a single data point, in which case the point in question was removed¹⁵.

A metric known as the σ_0 - π_0 distance is used to calculate how close two different water parcels are to each other in terms of physical properties referenced at sea surface, where σ_0 is potential density and π_0 is potential spicity¹². Contours of π_0 are orthogonal to those of σ_0 , hence π_0 contains information regarding temperature and salinity not included in the potential density. In contrast to θ -S space, the gradients in σ_0 - π_0 space are the same magnitude, allowing a meaningful calculation of distance. The σ_0 - π_0 distance between the densest overflow water ($\sigma_{0,1}$, $\pi_{0,1}$) and any upstream water parcel ($\sigma_{0,2}$, $\pi_{0,2}$) in the Nordic Seas is calculated by the following equation:

$$D_{1,2} = \sqrt{(\sigma_{0,1} - \sigma_{0,2})^2 + (\pi_{0,1} - \pi_{0,2})^2}.$$

The composite vertical sections were constructed using profiles from the historical

hydrographic dataset as follows. For each selected section, profiles with lateral distances less than 50 km from the line are used (grey crosses in Fig. 3a). The positions of profiles along the section are determined by the distance between their projected location (black crosses in Fig. 3a) and the location of the ridge (which is the origin of the section). The projected profiles are then gridded using Laplacian-spline interpolation²⁵. The final gridded sections have a horizontal resolution of 25 km and a vertical resolution of 25 m. The relative geostrophic velocities normal to the sections are calculated based on the gridded data. The absolute geostrophic velocities are obtained by using satellite-derived mean surface geostrophic velocity from 2005 to 2015 as the reference, which can be accessed at Copernicus Marine Environment Monitoring Service (CMEMS, http://marine.copernicus.eu).

253

254

255

243

244

245

246

247

248

249

250

251

252

Acknowledgements

- Funding for the study was provided by the US National Science Foundation under grants OCE-
- 256 1558742 (JH, RP) and OCE-1259618 (PL); the Bergen Research Foundation under grant
- 257 BFS2016REK01 (AB); and the National Natural Science Foundation of China No. 41576018 (FX)
- 258 and 41606020 (FX).

259

260

261

Author contributions

- JH, RP, and AB assembled and analyzed the data; RH developed the σ_0 - π_0 distance methodology
- and helped apply it; JH and RP wrote the paper and all authors interpreted the results and clarified
- the implications.

264 Competing interests

265 The authors declare no competing financial interests.

266 References

- 1. Hansen, B. & Østerhus S. North Atlantic–nordic Seas Exchanges, *Progress in oceanography* **45(2)**, 109-208 (2000).
- 269 2. Mauritzen, C. Production of dense overflow waters feeding the North Atlantic across the
 270 Greenland-Scotland Ridge. Part 1: Evidence for a revised circulation scheme, *Deep Sea Research Part I: Oceanographic Research Papers* 43(6), 769-806 (1996).
- 3. Våge, K. *et al.* Significant role of the North Icelandic Jet in the formation of Denmark Strait overflow water, *Nature Geoscience* **4(10)**, 723 (2011).
- 4. Mastropole, D. *et al.* On the hydrography of Denmark Strait, *Journal of Geophysical Research: Oceans* **122(1)**, 306-321 (2017).
- 5. Semper, S. *et al.* The emergence of the North Icelandic Jet and its evolution from northeast Iceland to Denmark Strait, *Journal of Physical Oceanography* **45**, 2499-2521 (2019).
- 6. Olsen, S. M., Hansen B., Quadfasel D. & Østerhus S. Observed and modelled stability of overflow across the Greenland–Scotland ridge, *Nature* **455(7212)**, 519 (2008).
- 7. Østerhus, S., Sherwin T., Quadfasel D. & Hansen B. The overflow transport east of Iceland, in Arctic–Subarctic Ocean Fluxes, edited, pp. 427-441, (Springer, Dordrecht, 2008).
- 8. Eldevik, T. *et al.* Observed sources and variability of Nordic seas overflow, *Nature Geoscience* **26**), 406 (2009).
- 9. Jeansson, E., Olsen A. & Jutterström S. Arctic Intermediate Water in the Nordic Seas, 1991-2009, *Deep Sea Research Part I: Oceanographic Research Papers* **128**, 82-97 (2017).
- 10. Dickson, R. R. & Brown J. The production of North Atlantic Deep Water: Sources, rates and pathways, *Journal of Geophysical Research* **C99**, 12319-12341 (1994).
- 288 11. Hansen, B. & Østerhus S. Faroe Bank Channel overflow 1995–2005, *Progress in Oceanography* **75(4)**, 817-856 (2007).
- 290 12. Huang, R. X., Yu L. S. & Zhou S. Q. New definition of potential spicity by the least square method, *Journal of Geophysical Research: Oceans* **123(10)**, 7351-7365 (2018).
- 292 13. Pickart, R. S., Torres D. J. & Clarke R. A. Hydrography of the Labrador Sea during active convection, *Journal of Physical Oceanography* **32(2)**, 428-457 (2002).
- 294 14. Marshall, J. & Schoot F. Open-ocean convection: Observations, theory, and models. *Reviews* of *Geophysics* **37**, 1-64 (1999).

- 15. Brakstad, A., Våge K., Håvik L. & Moore G. W. K. Water Mass Transformation in the Greenland Sea during the Period 1986-2016, *Journal of Physical Oceanography* **49**, 121-140 (2019).
- 16. Våge, K., Moore G. W. K., Jónsson S. & Valdimarsson H. Water mass transformation in the Iceland Sea, *Deep Sea Research Part I: Oceanographic Research Papers* **101**, 98-109 (2015).
- 17. Pickart, R. S. *et al.* The North Icelandic Jet and its relationship to the North Icelandic Irminger Current, *Journal of Marine Research* **75(5)**, 605-639 (2017).
- 303 18. Huang, J. *et al.* Structure and Varibility of the North Icelandic Jet From Two Years of Mooring Data, *Journal of Geophysical Research: Oceans* **124**, 3987-4002 (2019).
- 19. Harden, B. *et al.* Upstream sources of the Denmark Strait Overflow: Observations from a high-resolution mooring array, *Deep-Sea Research I* **112**, 94-112 (2016).
- 307 20. Hopkins, T.S., Baldasserini, G., Minnett, P., Povero, P. & Zanasca, P. Icelandic Current
 308 Experiment. GIN SEA Cruise 88 Data Report. Hydrography and Circulation. Tech. Rep.
 309 SM-260, Saclant Undersea Research Centre (1992). URL
 310 https://openlibrary.cmre.nato.int/handle/20.500.12489/212.
- 21. Yang, J. & Pratt L. J. Some dynamical constraints on upstream pathways of the Denmark Strait Overflow, *Journal of Physical Oceanography* **44(12)**, 3033-3053 (2014).
- 22. Olsson, K. A. *et al.* Intermediate water from the Greenland Sea in the Faroe Bank Channel: spreading of released sulphur hexafluoride, *Deep Sea Research Part I: Oceanographic Research Papers* **52**, 279-294 (2004).
- 23. Lauvest, S. L. *et al.* Continued warming, salinification and oxygenation of the Greenland Sea gyre. *Tellus* **70A**, 1-9 (2018).
- 318 24. Behrendt, A., Sumata H., Rabe B. & Schauer U. UDASH–Unified Database for Arctic and Subarctic Hydrography, *Earth System Science Data* **10(2)**, 1119-1138 (2018).
- 25. Pickart, R. S. & Smethie W. M. Temporal evolution of the deep western boundary current where it enters the sub-tropical domain, *Deep Sea Research Part I: Oceanographic Research Papers* **45**, 1053-1083 (1998).

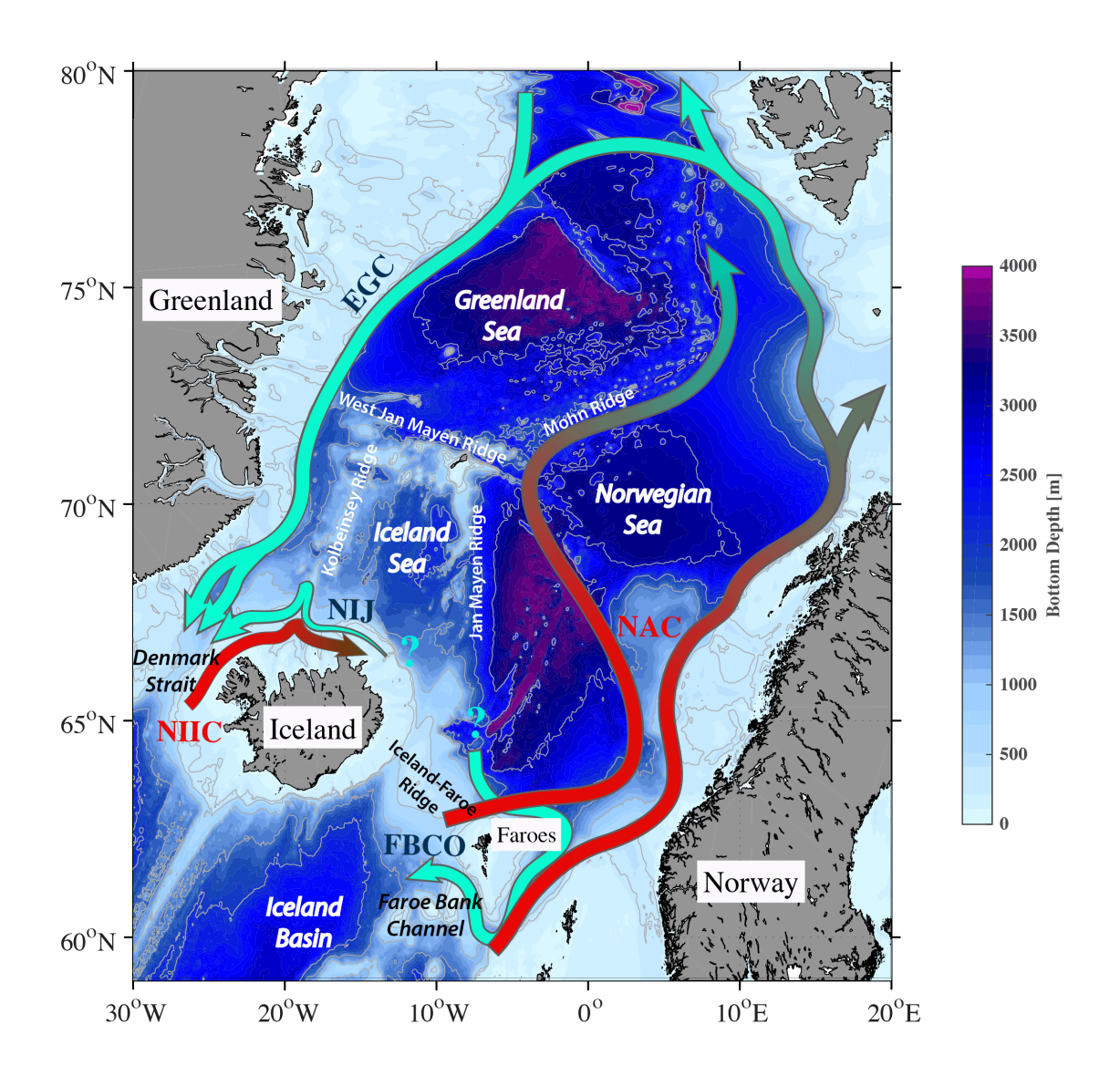


Figure 1| Schematic circulation of the Nordic Seas.

The pathways of warm Atlantic inflow and dense outflow are shown in red and green arrows, respectively. Colors and grey contours represent the bathymetry from ETOPO2, and the relevant ridges are named. The abbreviations are: NAC, Norwegian Atlantic Current; NIIC, North Icelandic Irminger Current; EGC, East Greenland Current; NIJ, North Icelandic Jet; FBCO, Faroe Bank Channel overflow. Question marks denote uncertainty in upstream the source/pathways of the dense overflows.

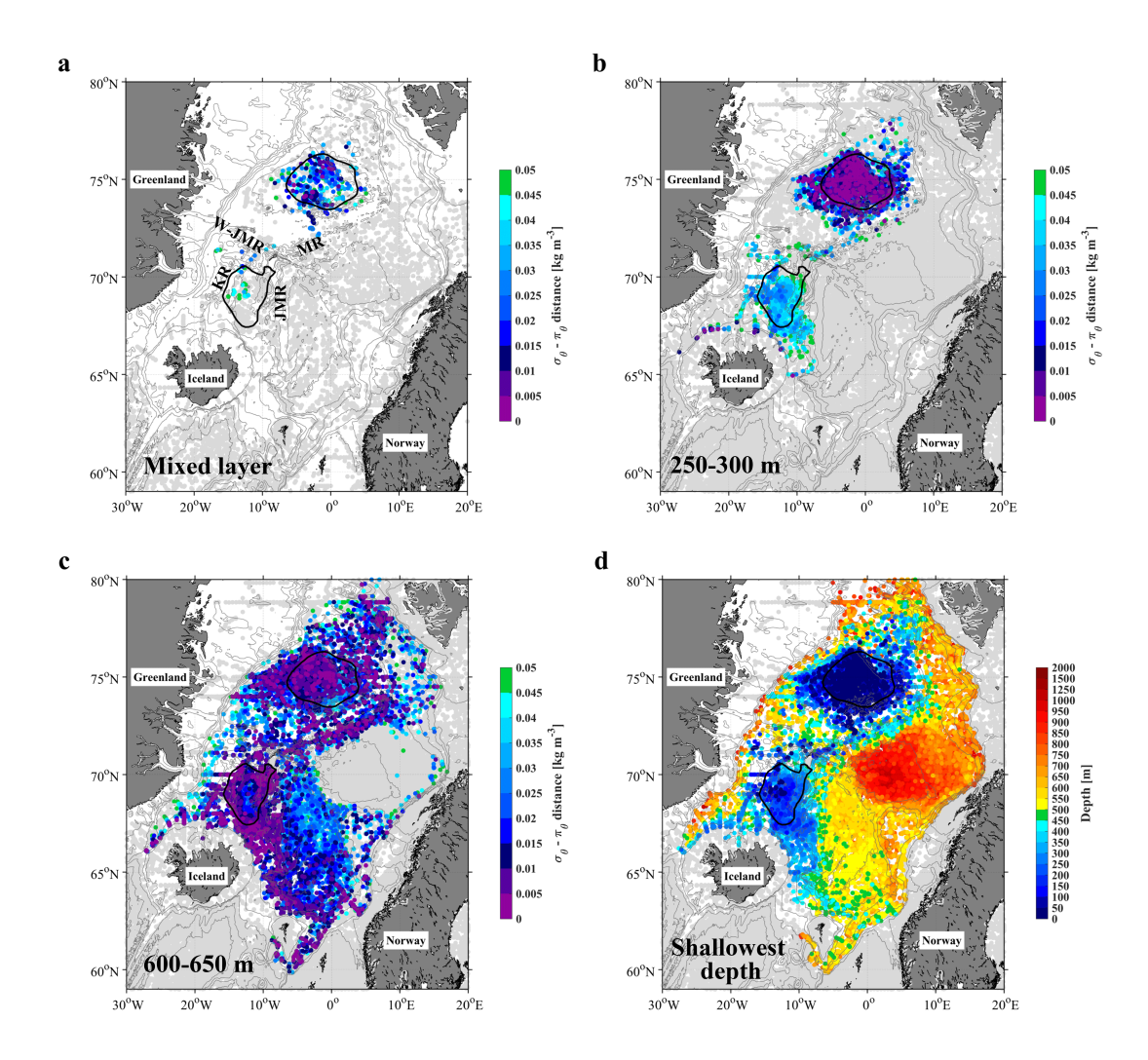


Figure 2| Proximity in water mass space to the densest overflow water.

(a) Distribution of the small potential density – potential spicity (σ_0 - π_0) distances ($\leq 0.05 \text{ kg m}^{-3}$) for late-winter (February-April) mixed layers from 2005 to 2015. Distances > 0.05 kg m⁻³ are shown by light-grey circles. The Greenland Sea and Iceland Sea gyres are delimited by the 4.5 and 7 dynamic cm contours, respectively, of sea surface dynamic height relative to 500 db (thick black contours). The thin grey contours show the bathymetry from ETOPO2, with four ridges labeled: MR, Mohn Ridge; W-JMR, West Jan Mayen Ridge; JMR, Jan Mayen Ridge; KR, Kolbeinsey Ridge. (b and c) The year-round distribution of small σ_0 - π_0 distances in the 250-300 m layer and 600-650 m layer, from 2005 to 2015. (d) The shallowest depth at which a small σ_0 - π_0 distance value (0.05 kg m⁻³) is first found in the vertical. Stations where this value is not attained are shown by light-grey circles.

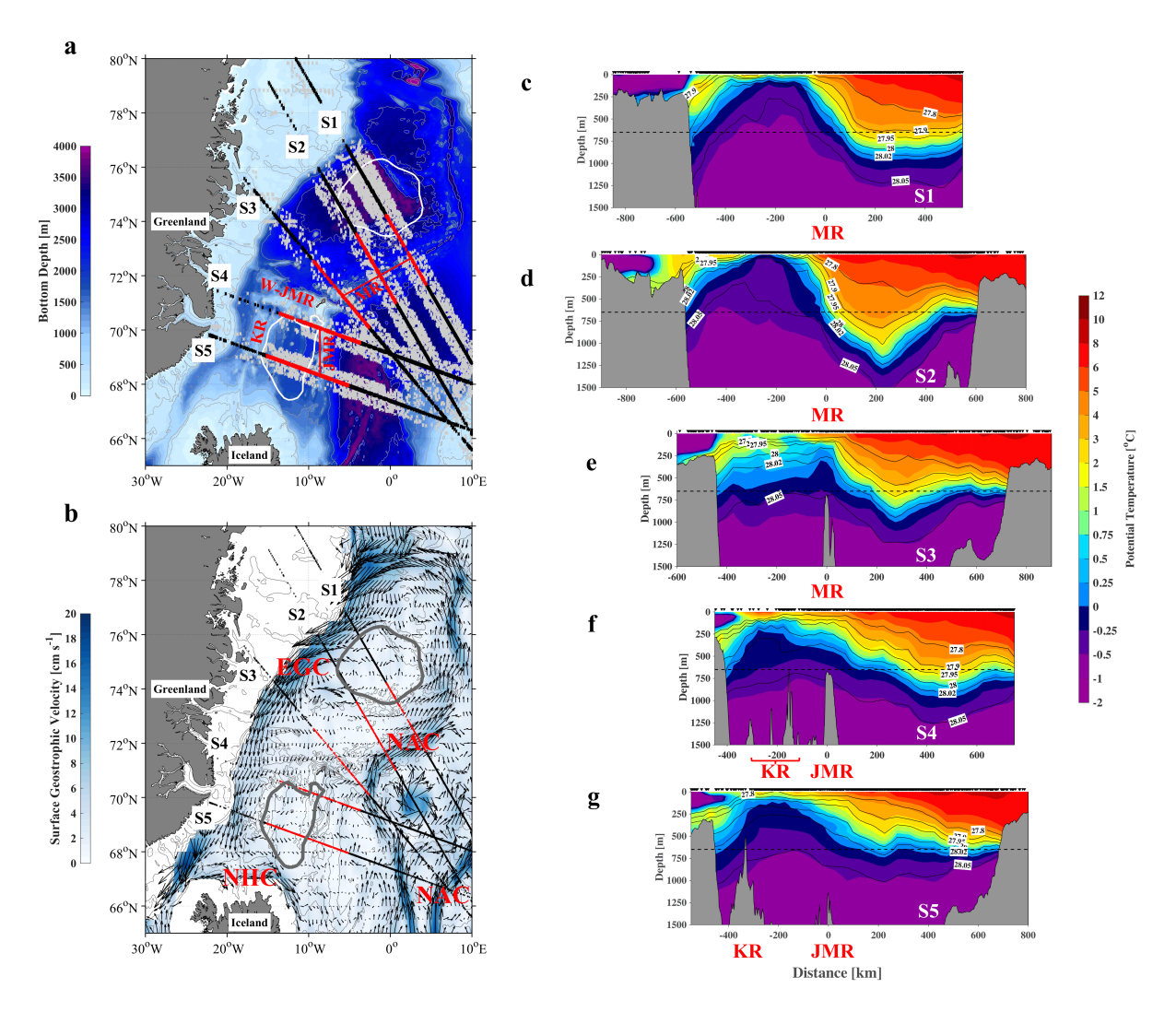


Figure 3 Cross-pathway sections of potential temperature and potential density.

(a) Locations of the five composite sections (S1-S5) centered on the Mohn Ridge (MR) and Jan Mayen Ridge (JMR). The original and projected locations of hydrographic profiles used in each section are indicated by grey and black crosses, respectively. The red crosses denote the segment of the section used for calculating the absolute geostrophic velocity in Figure 4. The Greenland Sea and Iceland Sea gyres are outlined by the white contours. (b) The long-term mean (2005-2015) surface geostrophic velocity from the gridded satellite altimeter product. The two branches of the Norwegian Atlantic Current (NAC), the East Greenland Current (EGC), and the North Icelandic Irminger Current (NIIC) are labeled. The color indicates speed [cm s⁻¹]. (c-g) Cross-sections of potential temperature [°C], overlain by potential density contours [kg m⁻³]. The origin of the x axis in S1-S3 and in S4-S5 are the locations of Mohn Ridge and Jan Mayen Ridge, respectively. The horizontal dashed back line indicates the sill depth of Denmark Strait (650 m).

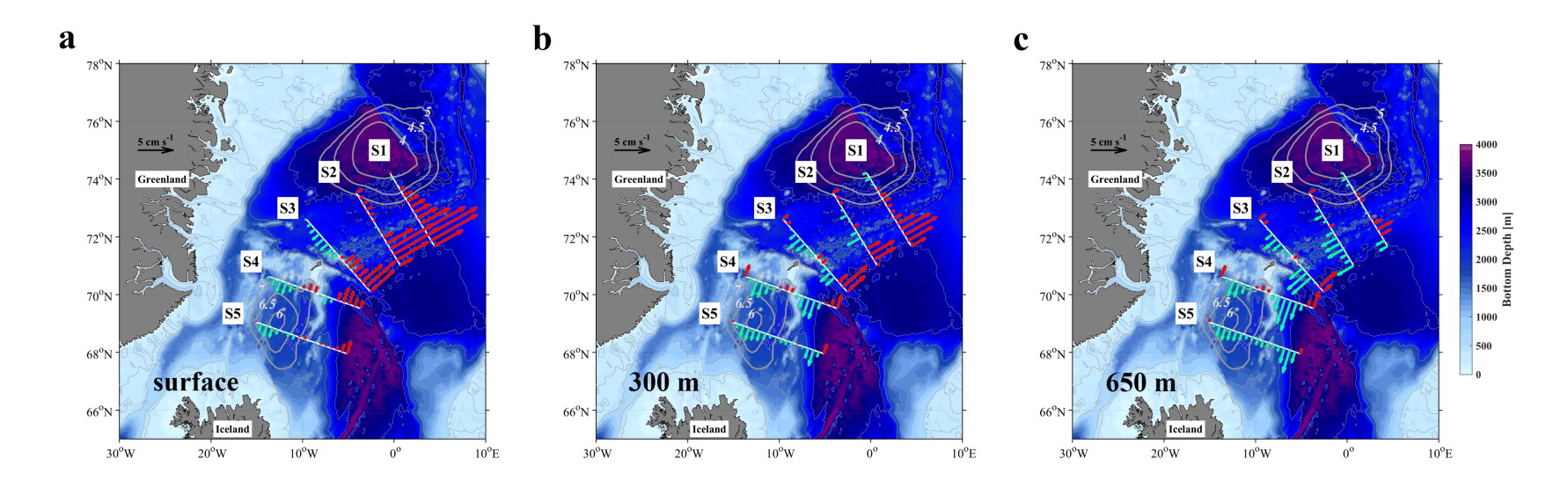


Figure 4 Velocities along the pathways.

Absolute geostrophic velocity [cm s⁻¹] normal to the five composite sections for (a) the surface, (b) 300 m, and (c) and 650 m, calculated using the hydrographic data and the satellite-derived surface geostrophic velocity in Figure 3. The southward and northward flows in each section are shown in blue and red, respectively. The Greenland Sea and Iceland Sea gyres are indicated by contours of sea surface dynamic height relative to 500 db in units of dynamic cm (thick grey contours).

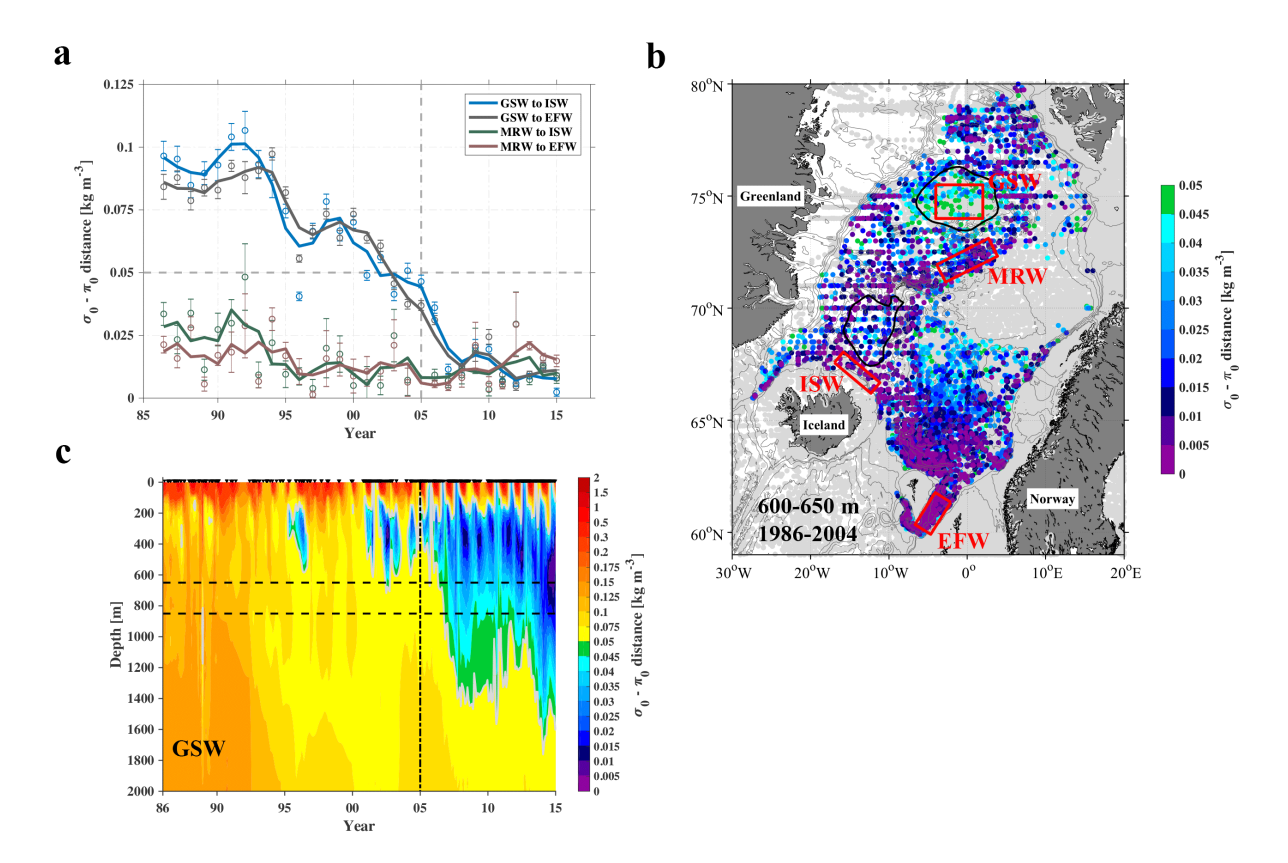
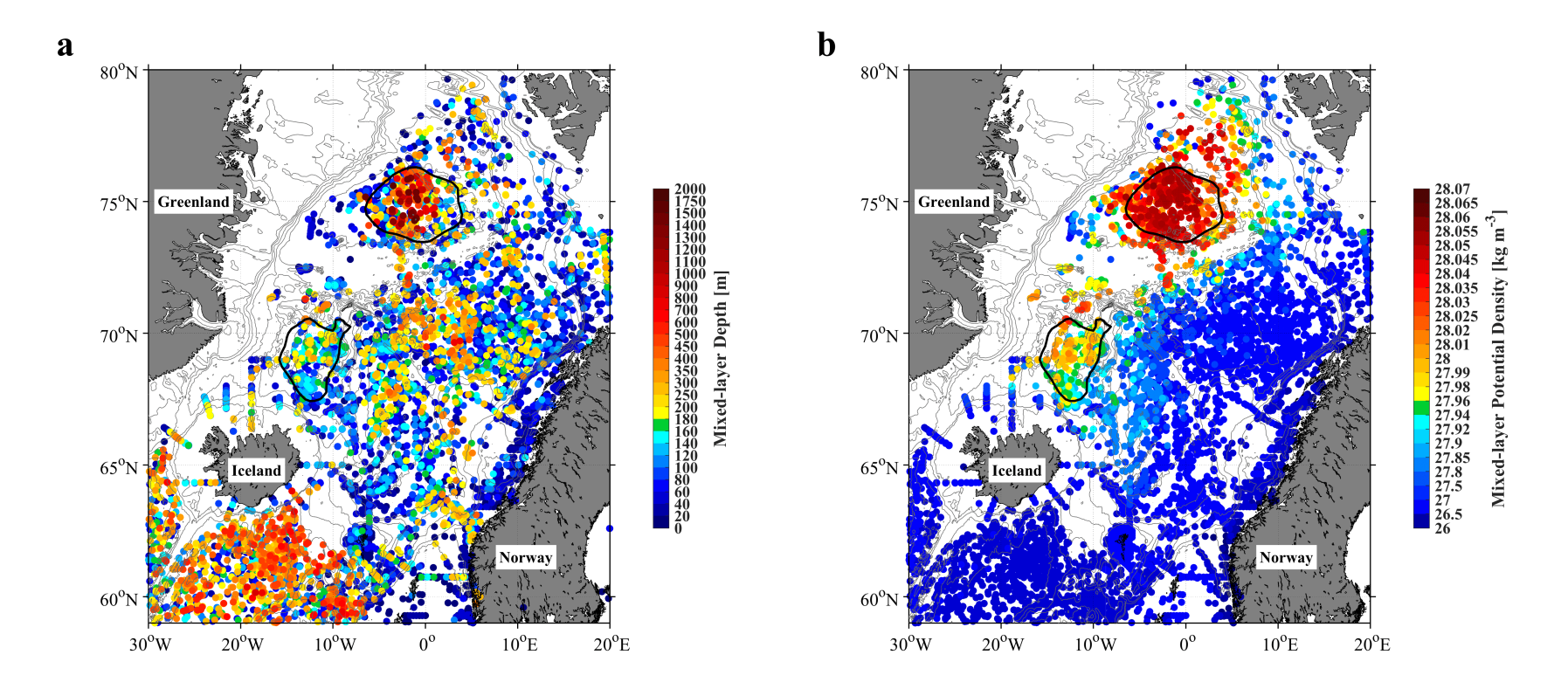


Figure 5 Long-term variability of the densest overflow water.

(a) Three-year running mean of σ_0 - π_0 distances between the densest overflow water (28.03 $\leq \sigma_0$ ≤ 28.06 kg m⁻³, $\theta \leq 0$ °C and depth ≤ 850 m) in four geographical regions from 1986 to 2015: distance of GSW to ISW (blue solid line); GSW to EFW (grey solid line); MRW to ISW (green solid line); MRW to EFW (red solid line). The abbreviations are: Greenland Sea gyre water (GSW), Mohn Ridge water (MRW), North Iceland slope water (ISW), and East Faroes water (EFW). The four regions are outlined in Figure 5b. The solid circles are the annual means with error bars corresponding to the standard error. The vertical and horizontal dashed lines denote year 2005 and distance = 0.05 kg m⁻³, respectively. (b) Distribution of the small σ_0 - σ_0 distances between the time-varying NIJ transport mode and the water parcels in the 600-650 m layer, from 1986 to 2004. See text for details. (c) Evolution of σ_0 - σ_0 distances between the time-varying NIJ transport mode and the water within upper 2000 m of the Greenland Sea gyre. The two horizontal dashed lines indicate the sill depths of Denmark Strait (650m) and the Faroe Bank Channel (850m). The vertical dashed line denotes year 2005. The grey contours denote σ_0 - σ_0 distances = 0.05 kg m⁻³.

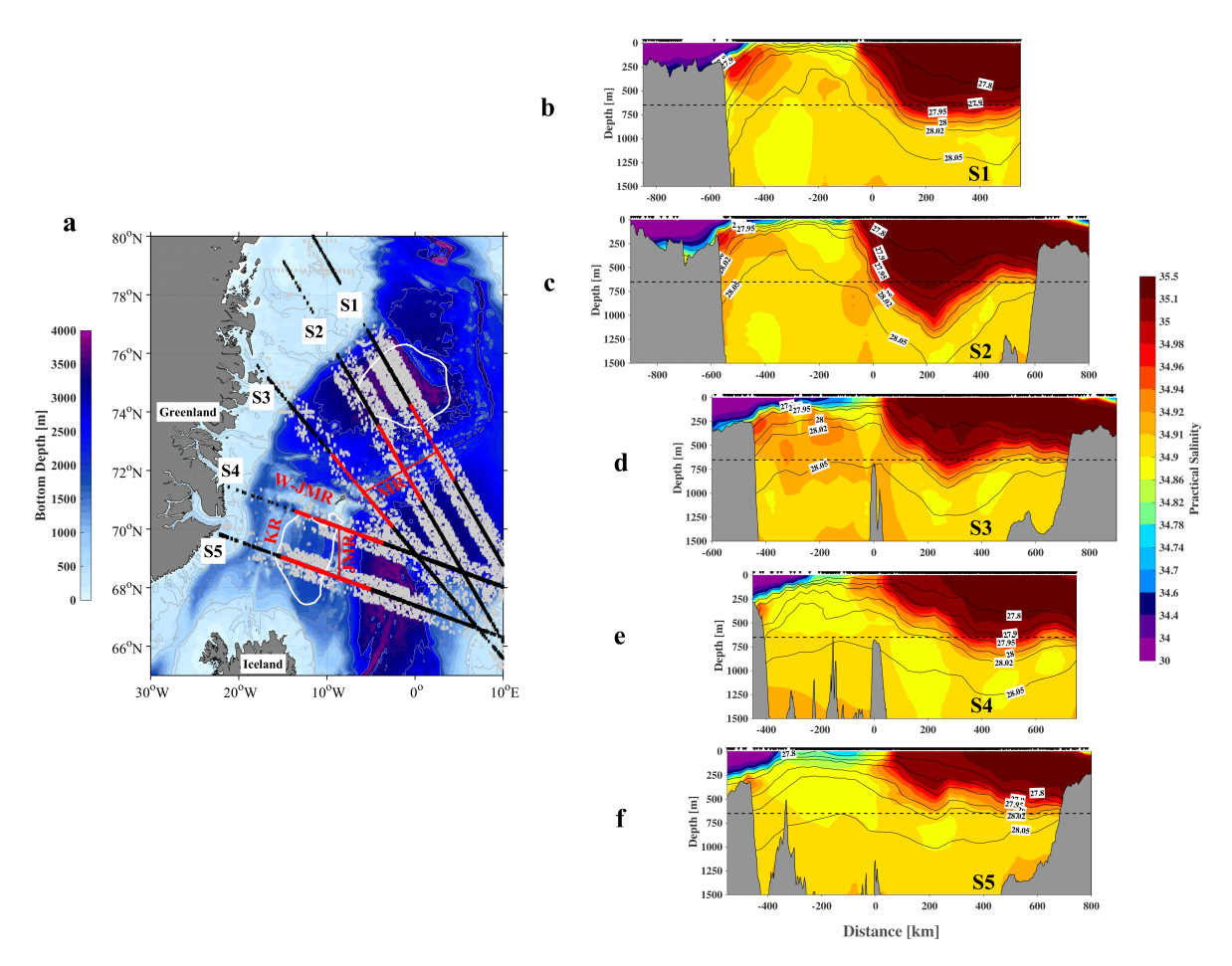
378 Supplementary Table 1 | Data sources with corresponding time periods and references.

Data source	Years	Reference
UDASH (Unified Database for Arctic	1980-	Behrendt et al., (2018)
and Subarctic Hydrography)	2015	https://doi.pangaea.de/10.1594/PANGAEA.872931
ICES (International Council for the	1980-	Data web page:
Exploration of the Seas)	2015	http://ocean.ices.dk/HydChem/HydChem.aspx
WOD (World Ocean Database)	1980-	Data web page:
	2015	www.noaa.gov/cgi-bin/OS5/SELECT/builder.pl
Argo float program	2001-	Data web page:
	2015	https://doi.org/10.17882/42182
NISE (Norwegian Iceland Seas	1980-	Nilsen et al., (2008), The NISE dataset, Faroese
Experiment database)	2009	Fisheries Laboratory Tech. Rep. 08-01, 20pp
MFRI (Marine Freshwater and	1980-	https://sjora.hafro.is
Research Institute of Iceland)	2015	
GLODAPv2 (Global Ocean Data	1980-	Olsen et al., (2019)
Analysis Project version 2) - 2019	2013	https://doi.org/10.5194/essd-11-1437-2019
		https://doi.org/10.25921/xnme-wr20

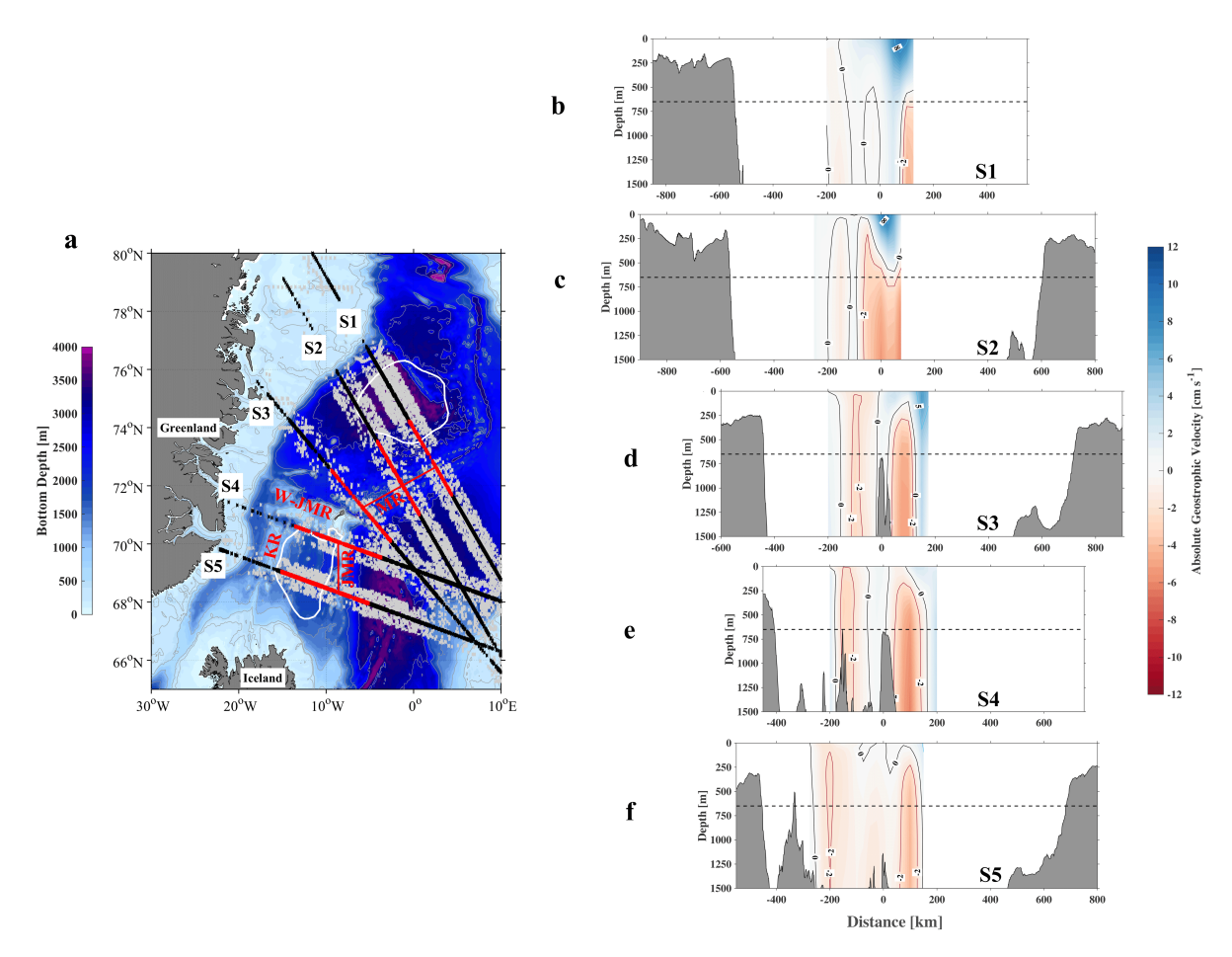


Supplementary Figure 1| Late-winter (February to April) mixed-layer properties.

(a) Late-winter mixed-layer depth [m] and (b) mixed-layer potential density [kg m⁻³]. The Greenland Sea and Iceland Sea gyres are outlined by thick black contours (see caption to Fig. 2). The thin grey contours show the bathymetry from ETOPO2.



Supplementary Figure 2 | Same as Figure 3 except for salinity.



Supplementary Figure 3 | Same as Figure 3 except for absolute geostrophic velocity.

Negative velocities are equatorward.